Modeling the combined impact of future climate and land use changes on streamflow of Xinjiang Basin, China

Renhua Yan, Jiacong Huang, Yan Wang, Junfeng Gao and Lingyan Qi

ABSTRACT

The response of hydrologic circulation to climate and land use changes is important in studying the historical, present, and future evolution of aquatic ecosystems. In this study, the Coupled Model Inter-comparison Project Phase 5 multi-model ensemble and a raster-based Xin'anjiang model were applied to simulate future streamflows under three climate change scenarios and two land use/cover change conditions in the Xinjiang Basin, China, and to investigate the combined effect of future climate and land use/cover changes on streamflow. Simulation results indicated that future climate and land use/cover changes affect not only the seasonal distributions of streamflow, but also the annual amounts of streamflow. For each climate scenario, the average monthly streamflows increase by more than 4% in autumn and early winter, while decreasing by more than −26% in spring and summer for the 21st century. The annual streamflows present a clear decreasing trend of −27%. Compared with land use/cover change, climate change affects streamflow change more. Land use/cover change can mitigate the climate change effect from January to August and enhance it in other months. These results can provide scientific information for regional water resources management and land use planning in the future.

Key words | impacts of climate and land use/cover changes, modeling, multi-model ensemble, raster-based Xin'anjiang model, streamflow, Xinjiang Basin

Renhua Yan
Jiacong Huang
Yan Wang
Junfeng Gao (corresponding author)
Lingyan Qi
Key Laboratory of Watershed Geographic Sciences,
Nanjing Institute of Geography and Limnology,
Chinese Academy of Sciences,
Nanjing 210008,
China
E-mail: *gaojunf@niglas.ac.cn*

Renhua Yan
University of Chinese Academy of Sciences,
Beijing 100049,
China

INTRODUCTION

Regional hydrologic cycle change is highly related to water scarcity, which has become a serious problem worldwide (Guo *et al.* 2008; Ouyang *et al.* 2014). Thus, evaluating the future variation of hydrologic cycle and water resources has special significance for regional planning and water resources management (Kiely 1999). Over the past 130 years, the climate system has experienced significant change. For instance, global average temperature has increased by 0.85 °C (IPCC 2013). Given the close relationship between the climate system and hydrologic circulation, climate change can have an impact on evapotranspiration and streamflow generation processes within the catchment, thereby affecting regional water quantity and quality in rivers. Moreover, with population growth, increasing human activities (e.g., land use/cover change and irrigation) as an external force exerts more and more influences on the hydrology cycle. Therefore, inquiring how climate and land use/cover change affect the seasonal and annual characteristics of hydrological variables is important in projecting the future variation of hydrology and water resources. Some previous studies have focused on the impact of climate or land use/cover change on the hydrologic cycle in the historical or current period by using historical hydro-climatic data (Wisser *et al.* 2010; Agrawal *et al.* 2014; Hallema *et al.* 2014; Niedda *et al.* 2014; Rouge & Cai 2014). However, the combined effect of future climate and land use/cover changes has received relatively less attention. On the other hand, with regard to the effect of

doi: 10.2166/nh.2015.206

land use/cover change, few studies have investigated the response of three streamflow components (i.e., surface, interflow, and groundwater runoff) to future land use/cover change (Guo *et al.* 2008).

Global climate models (GCMs) provide one of the best tools for simulating the future climate change (Arora & Boer 2001; Arnell *et al.* 2004; Manabe *et al.* 2004; Xu *et al.* 2010). Thus, many climate models such as CGCM3.1 (Tu 2009), ECHAM (Kalantari *et al.* 2014), HadCM3 (Ouyang *et al.* 2014) models, have been applied to provide future climate datasets for estimating the effects of climate change on streamflows over the last 20 years. Afterwards, the multi-model ensemble has been extensively used to reduce the biases and uncertainties of future climate simulation from a single climate model (Jarsjo *et al.* 2012; Sun *et al.* 2013; Lopez-Moreno *et al.* 2014). Overall the multi-model ensembles applied in the previous studies on the regional hydrological effects of future climate change were mainly derived from the simulation of GCMs participating in the Coupled Model Intercomparison Project Phase 3 (CMIP3). More recently, CMIP5 dataset under representative concentration pathway (RCP) scenarios have been used to analyze the temporal and spatial changes of temperature and precipitation over China in the 21st century (Xu & Xu 2012; Tian *et al.* 2015). Compared to CMIP3, CMIP5 has adopted a much more coordinated approach to generate uniform inputs, standardized outputs, and a more systematic storage of the results in the climate modeling experiment (Smith *et al.* 2013). In this paper, a CMIP5 multi-model dataset was introduced to drive the hydrological model in the hope of accurate representation of future climate change in the study area.

The hydrological model is the principal tool used in investigating the hydrological processes and their responses to climate and land use/cover changes (Niedda *et al.* 2014). The conceptual lumped Xin'anjiang model is one of the most extensively used hydrological models for forecasting streamflow in the humid and semi-humid regions of China (Tian *et al.* 2013; Li *et al.* 2014; Yao *et al.* 2014). This study utilized the PCRaster software to develop a raster-based Xin'anjiang model that can represent the spatial variability of the hydrological processes. The PCRaster software was developed by Utrecht University (Van Deursen 1995), and has been widely used in hydrological and environmental modeling (Zhao *et al.* 2010; Huang *et al.* 2012, 2015). The raster-based Xin'anjiang model is a combined distributed/lumped model which is relatively simpler and less data-intensive compared to other distributed or semi-distributed hydrological models such as MIKE SHE model (Vansteenkiste *et al.* 2013) and SWAT model (Musau *et al.* 2015). Furthermore, most of the input data were available from online sources.

In this study, the developed raster-based Xin'anjiang model was used to simulate streamflow during 1990–2007 for calibrating and validating the model. Then, the calibrated Xin'anjiang model was employed to predict future streamflow changes under three climate change and two land use change scenarios in Xinjiang Basin based on the CMIP5 dataset. The objectives of this study are as follows: (1) analyze the seasonal and annual-averaged streamflow variations under climate change alone and land use change alone; (2) compare the sensitivity of streamflows to climate change and land use change; and (3) investigate the combined effect of climate and land use/cover changes on streamflow.

STUDY AREA AND DATA

Study area

The Xinjiang Basin (27 °33′–28 °59′N, 116 °23′–118 °22′E) is one of the five sub-basins of Poyang Lake Basin located in the lower reaches and the south bank of the Yangtze River (Figure 1). A portion of approximately 14.6% of Poyang Lake water (the largest freshwater lake in China) is supplied by the Xinjiang sub-basin (Xie *et al.* 2009), which accounts for 10.9% of the total Poyang Lake Basin area. Therefore, the hydrological response of Xinjiang Basin to future climate and land use/cover change directly affects the water level change of Poyang Lake. The catchment above Meigang hydrological gauging station has a drainage area of 1.53×10^4 km^2 between the southern foothills of Wuyi Mountain and north-facing slope of Huaiyu Mountain. Affected by the topography, the river flows primarily from the east to the west and enters Poyang Lake at Meigang. The multi-year averaged annual streamflow at Meigang station in 1990–2007 was 605.9 m^3/s, with mean monthly maximum

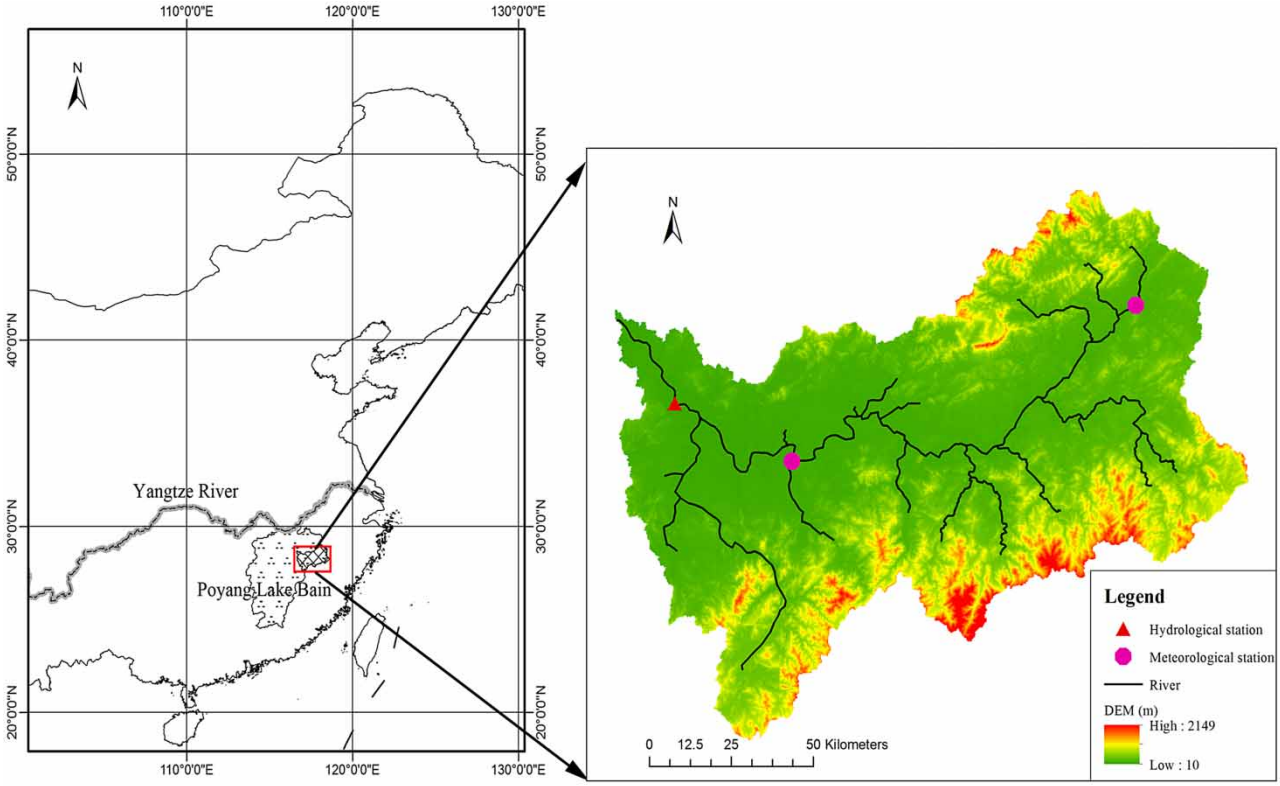

Figure 1 | Location of the Xinjiang Basin and hydrological and meteorological gauges.

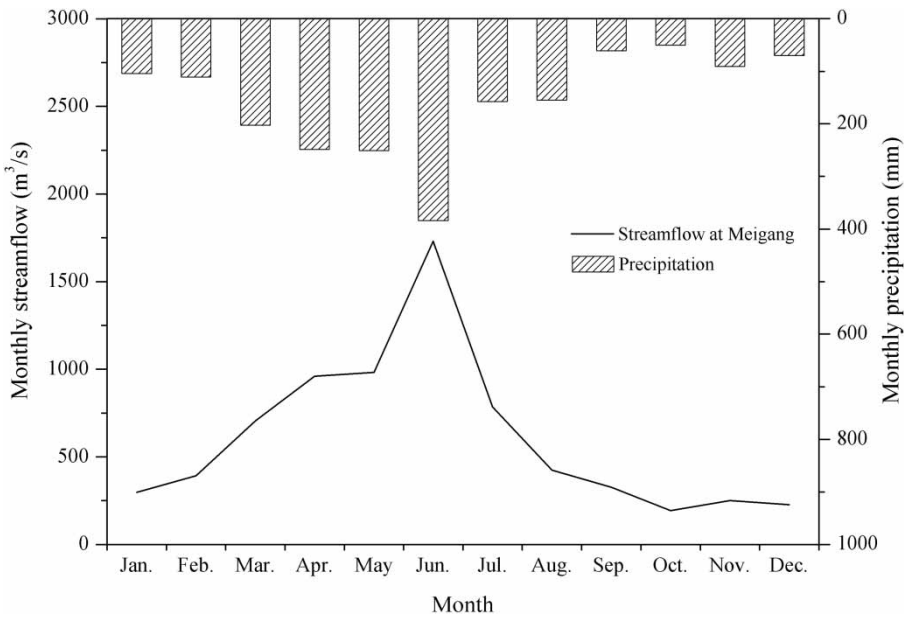

Figure 2 | Monthly streamflows and precipitation at Meigang station in Xinjiang Basin (1990–2007).

streamflow of 1,731.2 m^3/s in June and mean monthly minimum streamflow of 193.0 m^3/s in October (Figure 2).

The study area is a subtropical monsoon climate characterized by a mean annual precipitation of 1,878 mm and average surface evaporation of 1,044 mm. More than half of the annual rainfall occurs between April and June (Figure 2), when the annual mean temperature is 18 °C.

Data and processing

The datasets required in the study including digital elevation model (DEM), land use/cover, historical meteorological and streamflows data, and the future climate scenarios were derived from different sources and are described below.

Spatial datasets

Spatial datasets are as follows: (1) the 30×30 m Advanced Spaceborne Thermal Emission and Reflection Radiometer (ASTER) DEM for the catchment was derived from the International Scientific and Technical Data Mirror Site, Computer Network Information Center, Chinese Academy of Sciences (http://www.gscloud.cn); (2) land use/cover data with 1×1 km resolution for three time periods (1980, 1994, and 2001) were provided by the Environmental and Ecological Science Data Center for West China, National Natural Science Foundation of China (http://westdc.westgis.ac.cn). These data were employed to calculate the historical land use change rate, which was then used to establish future land use scenarios. The land cover data of the year 2001 were used in model calibration and validation. Land use/cover is reclassified into four groups, namely, paddy field, dryland (farmland and forest land), open water, and developed land (residential, commercial, industrial, and transportation land use), to run the Xin'anjiang model. All of the spatial data (land use and DEM) were regridded to the same resolution of 250 m for streamflow modeling.

Historical meteorological and streamflow data

The input meteorological datasets of the Xin'anjiang model are precipitation and evapotranspiration. Given the shortage of observed evapotranspiration, the daily potential evapotranspiration was calculated by the FAO Penman–Monteith (P-M) method using other meteorological data. The daily meteorological data of this catchment were downloaded from the China Meteorological Data Sharing Service System (http://cdc.cma.gov.cn/home.do). These data consist of daily precipitation (mm), sunshine hours (h), water vapor pressure (hPa), wind speed (m/s), average temperature (°C), maximum temperature (°C), minimum temperature (°C), and relative humidity (%) during 1989–2007 for Guixi (28.30 °N, 117.22 °E, elevation of 50 m) and Yushan (28.68 °N, 118.25 °E, elevation of 100 m) meteorological stations (marked in Figure 1). These data were interpolated to each 250×250 m cell of the basin by using the inverse distance weighted interpolation method. The daily streamflow data (m^3/s) measured at Meigang gauge station from 1989 to 2007 were used for the calibration and validation of the Xin'anjiang model.

Future climate scenarios

The outputs of 21 climate models under RCP scenarios were used as the climate change projections for this study. Table 1 lists the selective 21 CMIP5 models. A more detailed description can be obtained from http://pcmdi9.llnl.gov/esgf-web-fe/.

The Beijing Climate Center (BCC) has applied a downscaling interpolation method to interpolate these model outputs with different horizontal resolution to a common 1×1 ° grid and then simply averaged the 21 models outputs to derive the CMIP5 multi-model ensemble mean (Xu & Xu 2012). In this study, on the basis of observed meteorological data during 1989–2007, the processed multi-model ensemble mean was downscaled into a high resolution 0.25×0.25 ° grid for catchment-scale climate variables of Xinjiang Basin by using the statistical downscaling method (SDM) (Tisseuil *et al.* 2010) and generalized additive model (GAM) (Yang *et al.* 2012). The SDM was employed to describe the empirical relationships between the large-scale climate variable from GCMs outputs and local-scale catchment conditions, and the GAM to generate the local-scale climate variable of future climate scenarios based on the observed meteorological data. More details of methods can be found in Wu *et al.* (2014). This paper will

Table 1 | Details of the 21 CMIP5 models

Model name	Modeling center/group	Resolution
BCC Climate System Model version 1 (BCC-CSM-1)	BCC, China Meteorological Administration, China	128 × 64
Beijing Normal University Earth System Model (BNU-ESM)	The College of Global Change and Earth System Science (GCESS), BNU, China	128 × 64
Canadian Earth System Model version 2 (CanESM2)	Canadian Centre for Climate Modelling and Analysis, Canada	128 × 64
The Community Climate System Model version 4 (CCSM4)	National Center for Atmospheric Research, USA	288 × 192
Centre National de Recherches Météorologiques Climate Model version 5 (CNRM-CM5)	CNRM/Centre Européen de Recherche et Formation Avancées en Calcul Scientifique, France	256 × 128
Commonwealth Scientific and Industrial Research Organization Mark Climate Model version 3.6 (CSIRO-Mk3-6-0)	CSIRO in collaboration with Queensland Climate Change Centre of Excellence, Australia	192 × 96
Flexible Global Ocean-Atmosphere-Land System Model-grid version 2 (FGOALS-g2)	State Key Laboratory of Numerical Modeling for Atmospheric Sciences and Geophysical Fluid Dynamics, Institute of Atmospheric Physics, Chinese Academy of Sciences, and Tsinghua University, China	128 × 60
The First Institution of Oceanography Earth System Model (FIO-ESM)	FIO, State Oceanic Administration (SOA), Qingdao, China	128 × 64
Geophysical Fluid Dynamics Laboratory Climate Model version 3 (GFDL-CM3)	GFDL, National Oceanic and Atmospheric Administration, USA	144 × 90
Geophysical Fluid Dynamics Laboratory Earth System Model version 2 with Generalized Ocean Layer Dynamics (GOLD) code base (GFDL-ESM2G)	GFDL, National Oceanic and Atmospheric Administration, USA	144 × 90
Geophysical Fluid Dynamics Laboratory Earth System Model version 2 with Modular Ocean Model version 4.1 (GFDL-ESM2M)	GFDL, National Oceanic and Atmospheric Administration, USA	144 × 90
Goddard Institute for Space Studies Model E version 2 with Hycoml ocean model (GISS-E2-H)	GISS, National Aeronautics and Space Administration, USA	144 × 90
Goddard Institute for Space Studies Model E version 2 with Russell ocean model (GISS-E2-R)	GISS, National Aeronautics and Space Administration, USA	144 × 90
Met Office Hadley Centre Global Environment Models version 2 with the new atmosphere–ocean component model (HadGEM2-AO)	Jointly with Met Office Hadley Centre and National Institute of Meteorological Research (NIMR), Korea Meteorological Administration (KMA), Seoul, South Korea	192 × 145
Institut Pierre Simon Laplace Climate Model 5A-Low Resolution (IPSL-CM5A-LR)	IPSL, France	96 × 96
Model for Interdisciplinary Research on Climate-Earth System, version 5 (MIROC5)	Atmosphere and Ocean Research Institute (AORI), National Institute for Environmental Studies (NIES), Japan Agency for Marine-Earth Science and Technology, Kanagawa (JAMSTEC), Japan	256 × 128
Model for Interdisciplinary Research on Climate-Earth System (MIROC-ESM)	JAMSTEC, AORI, and NIES, Japan	128 × 64
Atmospheric Chemistry Coupled Version of Model for Interdisciplinary Research on Climate-Earth System (MIROC-ESM-CHEM)	JAMSTEC, AORI, and NIES, Japan	128 × 64
Max-Planck Institute Earth System Model-Low Resolution (MPI-ESM-LR)	MPI for Meteorology, Germany	192 × 96
Meteorological Research Institute Coupled General Circulation Model version 3 (MRI-CGCM3)	MRI, Japan	320 × 160
The Norwegian Earth System Model version 1 with Intermediate Resolution (NorESM1-M)	Norwegian Climate Centre, Norway	144 × 96

concentrate on three greenhouse gas and aerosol precursor emission scenarios, namely, RCP 2.6 (low emissions), RCP 4.5 (medium emissions), and RCP 8.5 (high emissions), to study future environment change. RCP 2.6, RCP 4.5, and RCP 8.5 represent a scenario in which radiative forcing reach 2.6 w/m^2, 4.5 w/m^2, and 8.5 w/m^2 and CO_2 concentration increase up to 490 ppmv, 650 ppmv, and 1,370 ppmv by 2100, respectively (Moss *et al.* 2010). Monthly precipitation, air temperature, maximum air temperature, and minimum air temperature were chosen for two periods: 2016–2050 and 2051–2100 under these scenarios in this study. Then, the WXGEN weather generator model (Sharpley & Williams 1990) was utilized to generate daily meteorological data for simulating future daily streamflow and evapotranspiration.

Land use/cover change scenarios

Statistics show that the land use/cover change of Xinjiang catchment is chiefly the conversion of paddy field and dryland to developed land, especially residential land (Guo *et al.* 2008). It was assumed that this trend will continue in the future. Thus, the establishment of future land use/cover change scenarios will be based on the historical change of developed land use for three time periods (1980, 1994, and 2001). First, current land use change rate was derived from a regression of the percentage of developed land use (PDLU). Second, three future land use change scenarios were established: (1) constant-PDLU will be changeless, and the 2001 land cover data will be used for two future periods; (2) current rate-PDLU will increase at the current rate; and (3) double rate-PDLU will increase at the double current rate. Finally, future PDLU and percentages of other land use groups were calculated for each land use change scenario (Table 2).

This study spanned the period of 1990–2007 for the base years and covered two future periods, namely, 2016–2050 and 2051–2100.

MODEL

Model description

In this study, the distributed Xin'anjiang model conceptually based on the Xin'anjiang model was developed using PCRaster at a daily timescale. The core concept of the Xin'anjiang model is runoff formation on the repletion of storage capacity (Yao *et al.* 2014). The model structure comprises four major modules, namely, evapotranspiration, runoff production, runoff separation, and flow routing (Zhao 1992). Compared with the previous version, some aspects of the Xin'anjiang model in this study have been revised as follows: (1) in the evaporation module, pan evaporation is substituted by the reference evapotranspiration (ET_o) by using the FAO P-M method (Allen *et al.* 1998; Cai *et al.* 2007) because of the lack of pan evaporation; (2) in the flow routing module, the surface runoff is routed using the one-dimensional 2kinematic wave function with Manning's equation within each sub-basin or in the channel instead of the unit hydrograph or Muskingum method. The interflow and groundwater are simulated by a simple linear storage. Table 3 lists the model parameters and their physical meanings.

For model calibration and validation, the trial-and-error method was adopted which is the same as that used in some previous Xin'anjiang model studies (Zhao *et al.* 2010; Lu *et al.* 2013), based on the daily results. After the initial warm-up period (year 1989), the measured daily streamflows

Table 2 | Current and future land use conditions of Xinjiang Basin

Land use type	Open water	Paddy field	Developed land	Dryland	Developed land under the 'current rate' scenario		Developed land under the 'double rate' scenario	
Year	2001	2001	2001	2001	2025	2075	2025	2075
Percentage (%)	1.5	28.4	1.2	68.9	4.3	10.0	7.2	18.5

Table 3 | Parameters of the raster-based Xin'anjiang model and calibrated values

Parameter	Physical meaning	Range[a]	Final value[c]
K_E	Ratio of potential evapotranspiration to calculated reference evapotranspiration in P-M method	Calibrated	1
B	Exponent of the distribution parabolic curve of tension water capacity	Catchment $<10\ km^2 = 0.1$; $\leq 300\ km^2 =$ 0.2–0.3; thousands $km^2 = 0.3$–0.4	0.4
WM	Areal mean tension water storage capacity	Varies from 80 mm in humid areas to 170 mm in arid areas	Paddyfield: 110 mm; Dryland: 120 mm
SM	Areal mean free water storage capacity	5–60 mm	60
Ex	Exponent of the distribution parabolic curve of free water capacity	1–1.5	1.4
KI	Outflow coefficient of the free water storage to interflow	KI + KG = 0.7–0.8	0.25
KG	Outflow coefficient of the free water storage to groundwater		0.45
KKI	Recession constant of lower interflow storage	0.5–0.9	0.8
KKG	Recession constant of groundwater storage	0.99–0.998	0.99
Beta	Parameter for momentum equation of kinematic wave	Calibrated	0.3
N	Manning's roughness coefficient	0.011–0.8[b]	0.8

[a]Suggested by Zhao (1992).
[b]Proposed by USDA-SCS (1986).
[c]Defined by calibration.

from 1990 to 2000 and from 2001 to 2007 at Meigang station were applied to calibrate and validate the model parameters, respectively (Table 3). The Nash–Sutcliffe coefficient (E_{NS}) and coefficient of determination (R^2) were utilized to evaluate the goodness of fit between the simulated and observed streamflows.

Model experiments

Simulation experiments of streamflows for three time periods in Xinjiang Basin were designed and conducted to study the effects of climate and land cover/use changes on the hydrological process. The three time periods are described as follows: (1) baseline period (1990–2007), in which model calibration and validation were done using the observed meteorological data and land use/cover data of year 2001; (2) future period of 2016–2050, in which the projected land use/cover data in 2025 were utilized; (3) future period of 2051–2100, in which the projected land use/cover data in 2075 were used. The climate and land use/cover data have to be altered for each of the three climate scenarios, each of the three land use/cover conditions, and each of the two future periods. As such, 18 model runs ($3 \times 3 \times 2$) have to be operated to reveal the effect of climate change alone, the effect of land cover/use change alone, and the combined effect of climate and land cover/use changes on future hydrological process.

RESULTS

Calibration and validation

Figures 3 and 4 graphically present the comparison of the simulated and observed streamflow values. Figure 3(a) shows that E_{NS} value was 0.83 for the daily streamflow during the calibration period. The magnitudes and fluctuations of the simulated daily streamflow values closely tracked the observed values well. Moreover, the trend of the temporal variation of streamflow was similar to that of precipitation intensity. This finding indicated that streamflow is mainly controlled by rainfall in Xinjiang Basin. The scatter diagram of the simulated and observed streamflow values was distributed along the 1:1 fit line, with the slope of the regression line (0.9103) close to 1

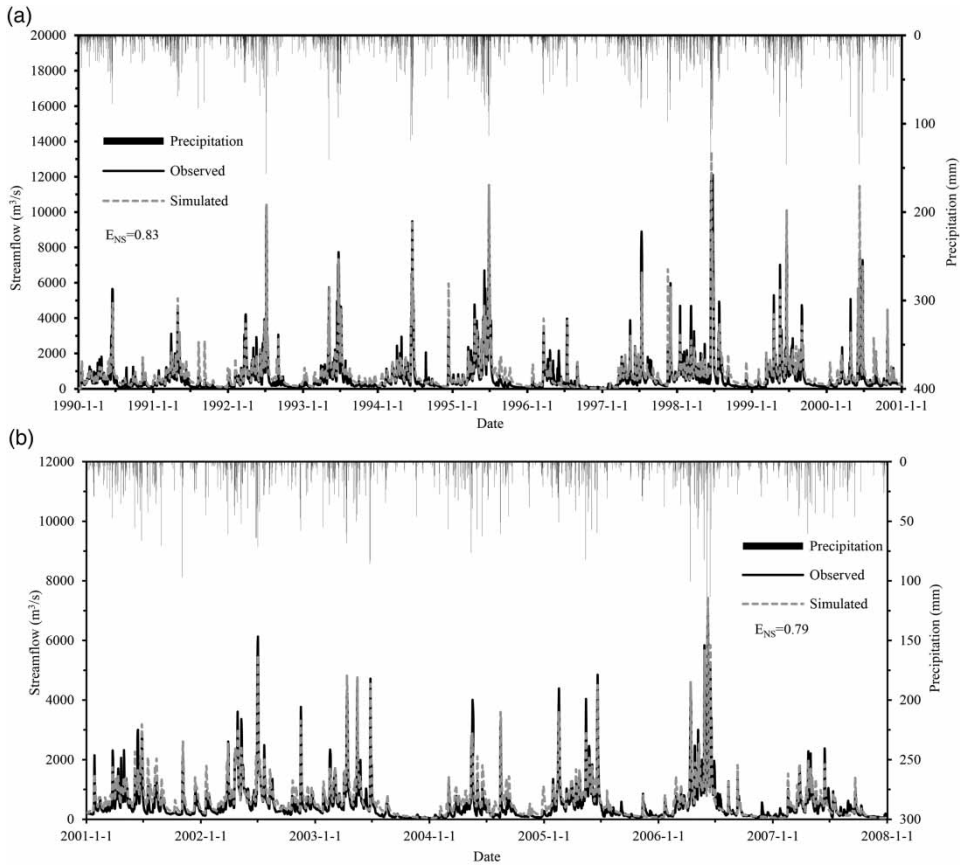

Figure 3 | Daily simulated and observed streamflow for model calibration (a) and model validation (b) at Meigang station.

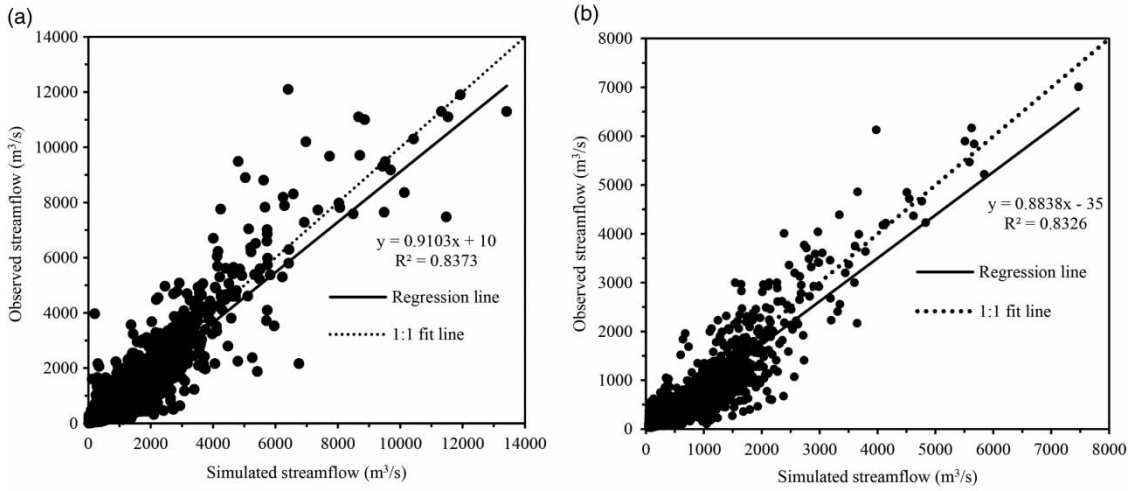

Figure 4 | Comparisons of the daily simulated and observed daily streamflows for model calibration (a) and model validation (b) at Meigang station.

(Figure 4(a)). R^2 was also up to 0.84 ($P < 0.001$), implying a close correlation between the observed and simulated streamflow values.

For model validation, E_{NS} and R^2 were calculated to be 0.79 and 0.83 ($P < 0.001$), respectively, indicating that the simulation results also capture the observed values

during 2001–2007, as well as the calibration results (Figure 3(b)). Furthermore, most of the scatter points were evenly distributed along the 1:1 fit line, with the slope of the regression line being close to 1 (Figure 4(b)). Thus, it was concluded that the Xin'anjiang model with the calibrated parameters can reasonably reflect the hydrological process in Xinjiang Basin (especially, given the larger catchment area, considerable interday variation in streamflow (12,093 m^3), and the sparse meteorological station). Therefore, the Xin'anjiang model can be applied to examine how future climate and land use/cover changes affect basin streamflow.

Impact of climate change on streamflow

Land use/cover is kept constant, i.e., the value is kept the same as in the baseline period, when the impact of climate change on streamflow was estimated alone. The simulated streamflow under constant land use condition and under different climate change scenarios including RCP2.6, RCP4.5, and RCP8.5 for the two periods (2016–2050 and 2051–2100) were used and compared with the corresponding values in the baseline period (1990–2007) (Figure 5).

Figure 5 shows that climate change has considerable impact on the monthly streamflow for the two future periods. In the autumn and early winter months (from September to December), the streamflows all increase under the three climate change scenarios. For instance, the modeled streamflows for the period of 2016–2050 increase by more than 20% compared with the baseline period in December. By contrast, streamflows in other months decrease substantially. In particular, streamflow in the early spring and early summer months (March and June) decrease approximately 40%. These results were consistent with the previous study of Sun *et al.* (2013), who used Soil and Water Assessment Tool model and six CMIP3 models to find the decrease in streamflows of the spring and summer months in the same region. This seasonal change of the climate effect might be explained by an increased precipitation in autumn and a decreased evapotranspiration in early winter due to the rapid decrease in temperature. This explanation can be proven by the comparison of precipitation, temperature, and potential evapotranspiration between the future periods and baseline period (Figure 6). In autumn (September and October), the average daily precipitation for the two future periods are higher than those for the baseline period, and the lower temperature results in lower potential evapotranspiration compared with those from the baseline period. Consequently, the increased net rainfall results in the larger streamflow for two periods. In later autumn and early winter (November and December), although precipitation decreases, the increase in water stored from the wetter autumn and a larger evapotranspiration reduction caused by the rapid decrease in temperature contribute to the increasing total streamflow. In contrast, in the later winter, spring, and summer months (from January to August), the large decrease in the average daily precipitation for the two future periods contributes to the decrease in rainfall-oriented streamflow, especially in the rainy season (from April to June), although the temperature slightly decreased in the period of 2016–2050.

Annual streamflows under the three climate scenarios for the future periods decreased by more than 20% from the baseline period (Figure 5), which also is the combined result of the decrease in annual precipitation, decreased temperature, and decreased evapotranspiration (Figure 6). Thus, climate change not only affects the seasonal change of streamflow, but also influences the amount of annual streamflows. This finding differs from that of eastern Massachusetts, USA (Tu 2009), where climate change mainly impacts the seasonal change of streamflow rather than the amount of annual streamflows. Compared with the continental climate in eastern Massachusetts (42 °21′N, 71 °10′W), the subtropical monsoon circulation of Xinjiang Basin is more easily affected by global climate change, thereby contributing to the substantial change in streamflow. Moreover, it can be inferred that precipitation generally affects streamflow change more than temperature and evapotranspiration, because the change trends of monthly and annual streamflows mostly correspond with that of precipitation. This finding is also proven by the correlation coefficients between climate factors change and streamflow change value, which implies that streamflow change is closely and significantly correlated with precipitation change (e.g., $R^2 = 0.72$, $P = 0.000$ under RCP4.5 for 2051–2100), whereas streamflow change is less correlated with temperature ($R^2 = 0.31$, $P = 0.060$ under RCP4.5 for 2051–2100) and potential evapotranspiration ($R^2 = 0.32$, $P = 0.055$ under RCP4.5 for 2051–2100).

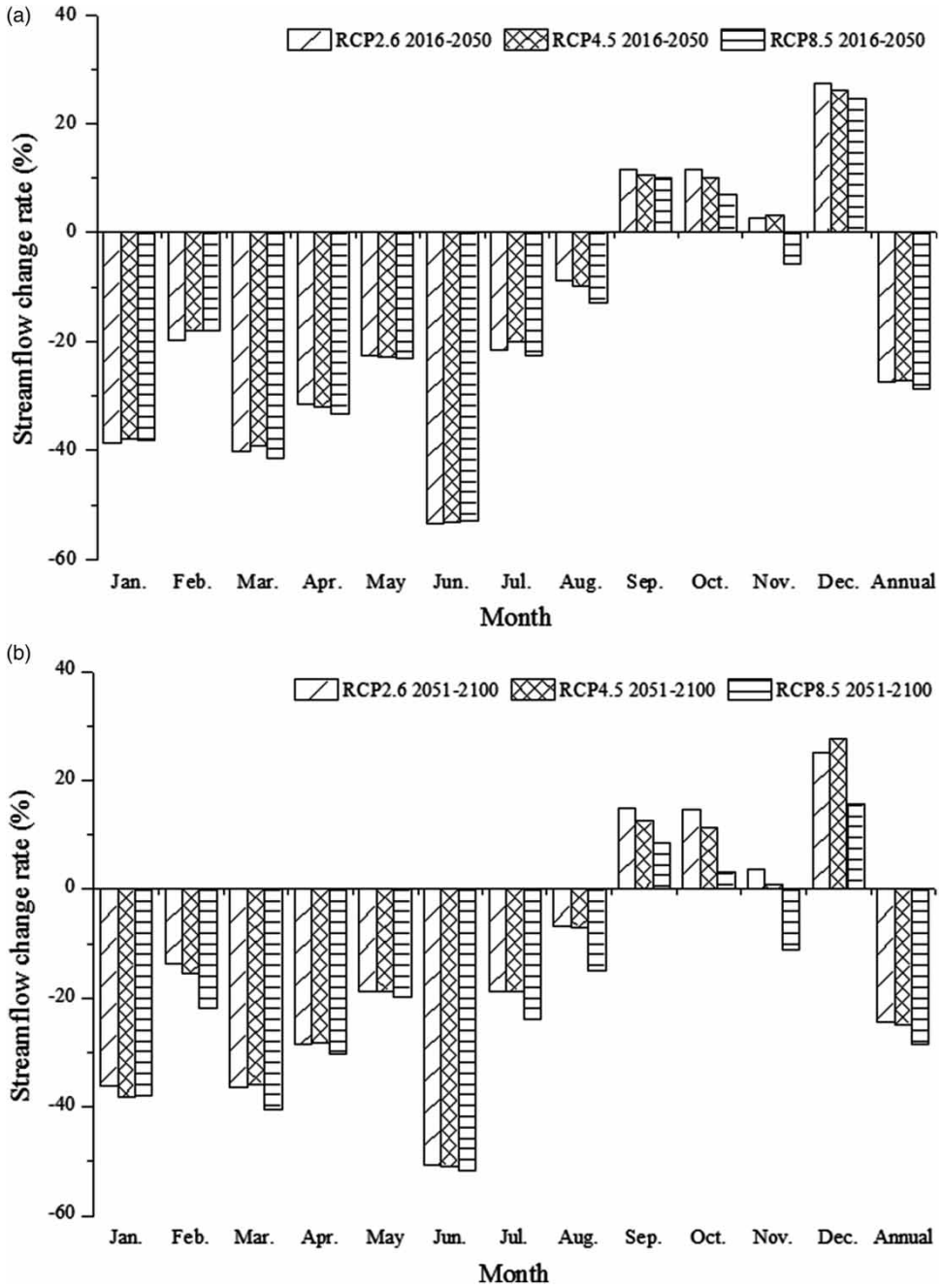

Figure 5 | Change in streamflows under the three future climate scenarios and 'constant' land use/cover condition from the current condition in the baseline period.

Among the three climate change scenarios, future streamflow changes have the same general pattern, although some differences are observed in individual months (Figure 5). The simulated streamflows for the period of 2016–2050 are similar to those for the period of 2051–2100. These results could be attributed to no substantial differences in precipitation, temperature, and evapotranspiration among the three climate scenarios and between the two future periods (Figure 6). In general, these climate scenarios have the same variation direction. Nevertheless, streamflows under the RCP8.5 climate scenario show a decreased trend in November due to the rapid decrease in

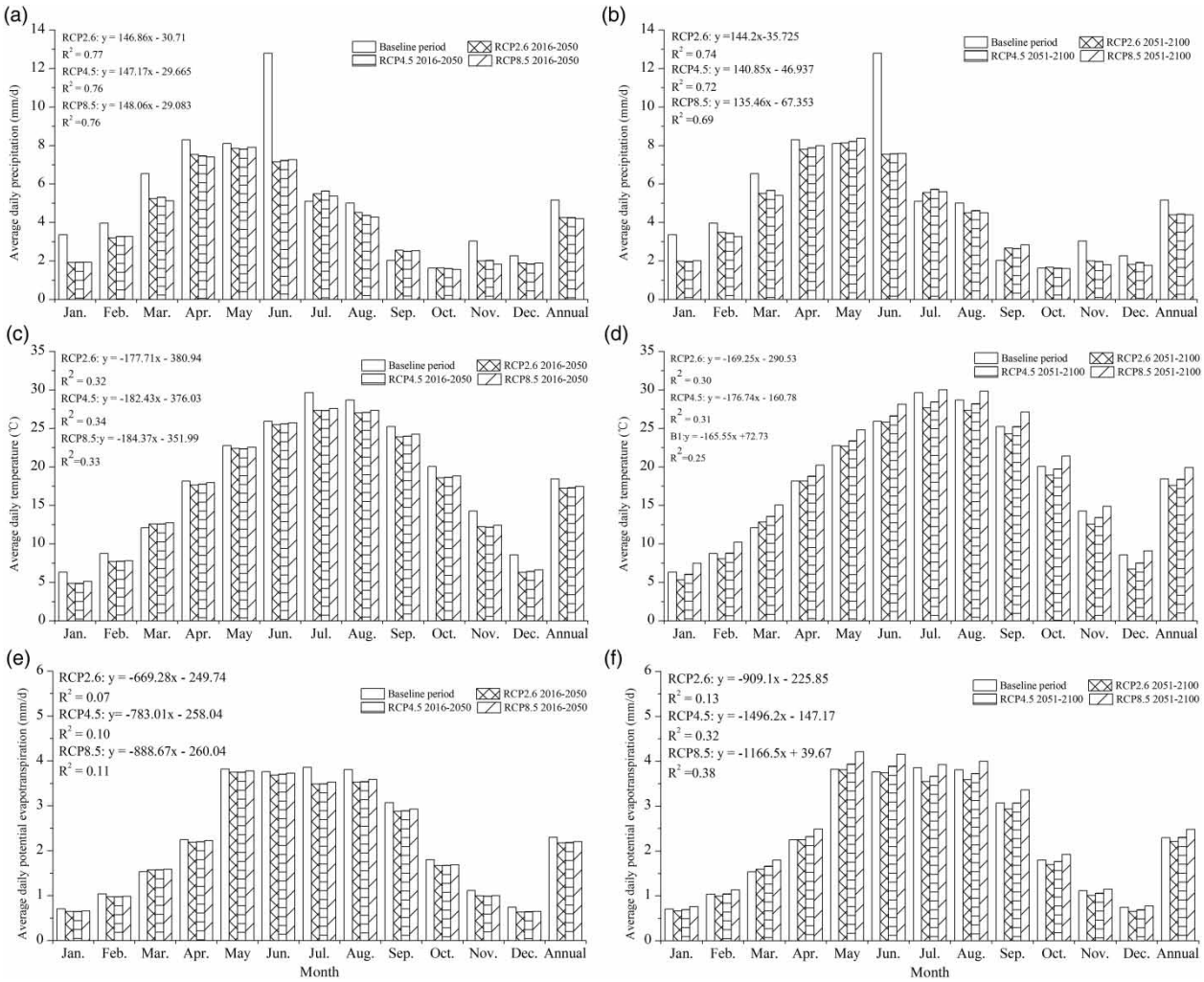

Figure 6 | Comparisons of daily precipitation (a), (b), temperature (c), (d), and potential evapotranspiration (e), (f) between the future periods and the baseline period, and their change value correlations with the change value of streamflow relative to baseline period.

precipitation (decrease by more than 40%) and slight increase in temperature, when compared with the increased trend of the other two climate scenarios.

Impact of land use/land cover changes on streamflow

Comparisons of the future streamflow under two different land use conditions but under the same climate change scenario are performed to evaluate only the effect of land use/land cover changes. In this section, only the simulated outputs under the RCP4.5 scenario are discussed because of the similar change trend of forecasted streamflows among the three different climate scenarios. Figure 7 shows the change in monthly and annual streamflows under the future 'current rate' and 'double rate' land use change conditions from the corresponding values under the 'constant' condition.

Figure 7(a) illustrates that future land use change significantly affects streamflow. A substantial increase in the simulated streamflow for the 'current rate' and 'double rate' conditions is observed throughout the year, which reaches its peak in March. For example, the increase rates of the simulated monthly streamflow vary from 0.4 to 9.3% for the period of 2016–2050 and from 1.7 to 25.8% for the period of 2051–2100 under the 'current rate' condition. The seasonal variation of the increase

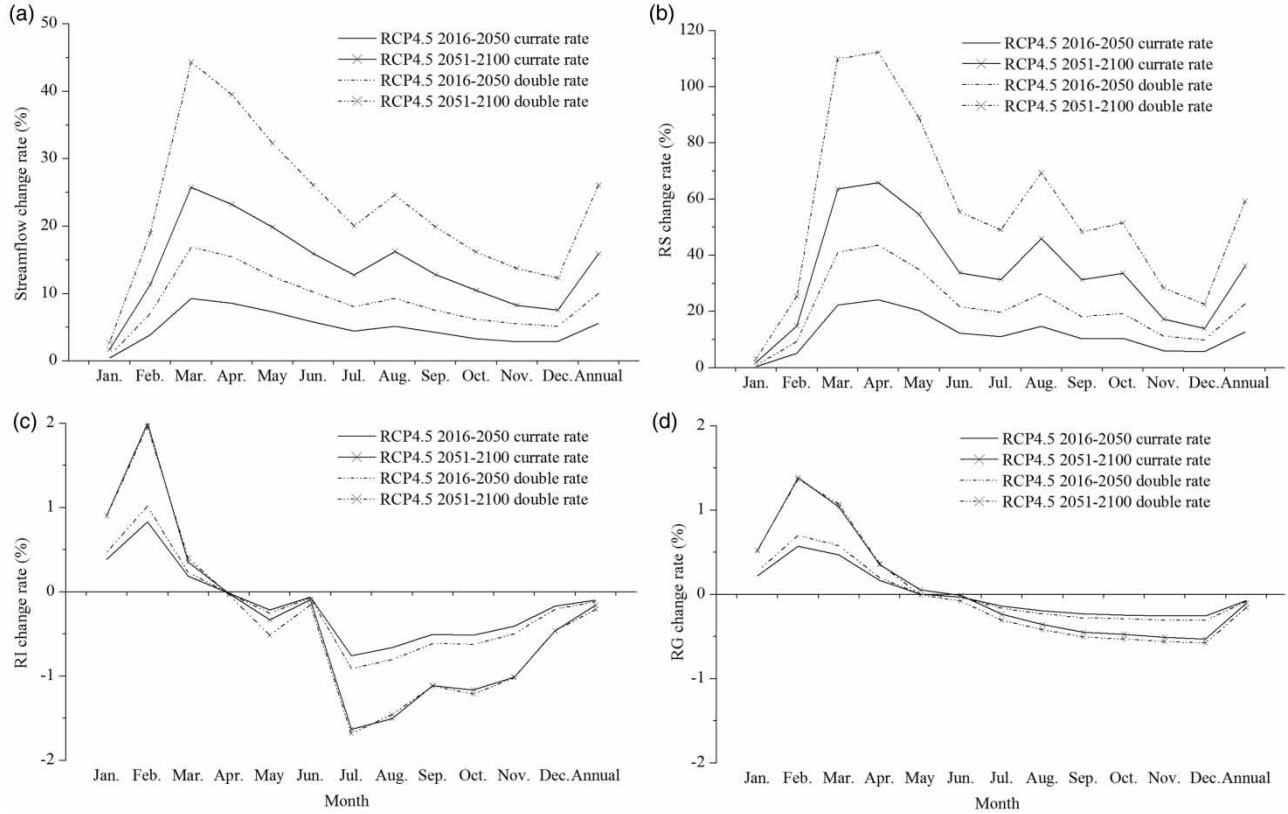

Figure 7 | Changes in streamflows (a) and their three components: surface runoff (RS) (b), interflow runoff (RI) (c), and groundwater runoff (RG) (d) under the RCP4.5 climate scenario and two future land use/cover conditions from the corresponding values under the 'constant' scenario.

rate implies that the spring (March, April, and May) and later summer (August) streamflows increase more compared with other seasons. With respect to the direction of streamflows change, in autumn and early winter, streamflows changes under the land use scenarios are identical to those affected by climate change alone. However, in later winter, spring, and summer, streamflows changes under the land use scenarios are opposite to those affected by climate change.

Since all monthly streamflows increase, the increase of annual streamflows is also found under the 'current rate' and 'double rate' condition for the two future periods (Figure 7(a)). This finding is contrary to the effect of climate change on the annual streamflows which indicated that the annual streamflow substantially decreased for the two future climate scenarios.

Considerable differences in the magnitude of future streamflow are observed between the 'current rate' and 'double rate' conditions. As shown in Figure 7(a), the monthly and annual streamflows under the 'current rate' condition are smaller than those under the 'double rate' condition. This result shows that rapid land development, i.e., a higher PDLU, can bring about a higher increase in streamflow. Some differences in streamflow are also observed between the periods of 2016–2050 and 2051–2100, even under the same future land use/cover scenario. Under the 'current rate' condition, the increase rate of annual streamflow for the period of 2016–2050 is 35% of that for the period of 2051–2100. Under the 'double rate' condition, the increase rate of annual streamflow for the period of 2016–2050 is 39% of that for the period of 2051–2100. These results indicate that, with the continued expansion of developed land, future streamflow will continue to increase.

Differences in hydrological response to land use/cover change are also observed among three streamflow components, namely, surface runoff (RS), interflow runoff (RI), and groundwater runoff (RG) (Figure 7(b)–7(d)). The monthly surface runoffs under the 'current rate' and 'double rate' scenarios are much higher than those under

the 'constant' scenario throughout the year, with a change trend that is mostly consistent with the streamflow (total runoff). Specifically, in April, the increase rate of surface flow under the 'current rate' and 'double rate' condition is up to 66%, and 112% for the period of 2051–2100, respectively. Furthermore, the annual surface runoff increases substantially with an average increase rate of 36% under the 'current rate' condition and 59% under the 'double rate' condition for the two future periods. Nevertheless, interflow and groundwater runoffs are less affected by land use/cover change. Under the two future land use/cover scenarios, the increase or decrease rate of monthly interflow and groundwater runoffs is smaller than 2% throughout the year for the two future periods. Although the rates increase from later winter to mid-spring (January to April) and decrease from early summer to early winter (July to December), the annual change rate is nearly zero. Thus, land use/cover change mainly affect the timing of interflow and groundwater rather than the amount of annual ones. This result shows that the larger increase in streamflow resulting from land use change is mainly caused by the increased surface runoff. This finding can be explained as follows: continued expansion of developed land leads to a larger reduction in evapotranspiration from the surface compared with the previously vegetated surface. On the other hand, continued expansion of developed land as impervious area, contributes to more water available for surface runoff and less available for interflow and groundwater. These changes induce higher surface runoff and higher net runoff yield. As for the effect of future land use change alone, flood potential will increase and become more destructive, especially in the rainy season.

Combined impact of climate change and land use/cover changes on streamflow

The simulated streamflows under the two land use change scenarios and under RCP4.5 climate scenario for the two future periods are compared with the corresponding current condition for the baseline period to investigate the combined effect of changes in climate and land use/cover, (Figures 8 and 9).

For most months of autumn and early winter, the streamflows increase substantially, with the rate ranging

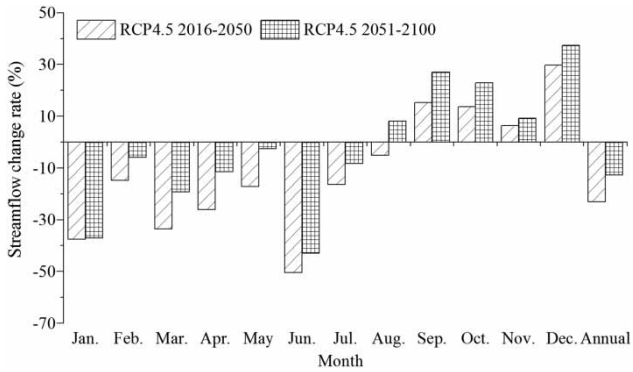

Figure 8 | Changes in streamflows under the RCP4.5 climate change and 'current rate' land use/cover scenarios from the current conditions in the baseline period.

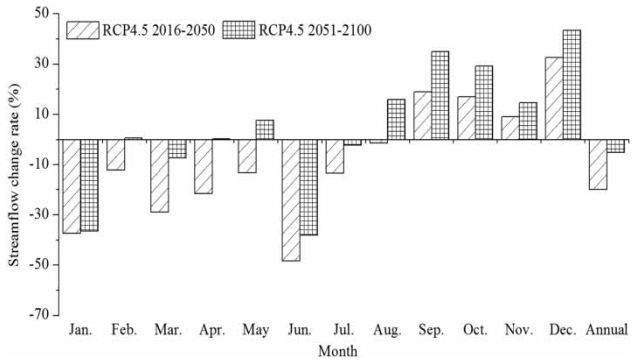

Figure 9 | Changes in streamflows under the RCP4.5 climate change and 'double rate' land use/cover scenarios from the current conditions in the baseline period.

from 6 to 43%, while for most months of later winter, spring, and summer, the streamflows decrease with the rate ranging from –2 to –50% (Figures 8 and 9). Therefore, combined with the previous analysis discussed in the sections Impact of climate change on streamflow and Impact of land use/cover changes on streamflow, the monthly streamflows under simultaneous climate and land use/cover change are consistent with that under climate change alone. This result shows that climate is the most sensitive boundary condition in the simulated future streamflow, that is, climate change plays a predominant role in controlling the future hydrologic cycle change in Xinjiang Basin, whereas the effect of land use/cover change is secondary. This finding is also in line with some previous studies (Lahmer *et al.* 2001; Legesse *et al.* 2003; Guo *et al.* 2008; Tu 2009), which found that climate change, especially precipitation, was the main driving factor of streamflow

changes in their respective study areas, rather than land use/cover change.

However, since the direction of the effect of land use/cover change is consistent with that of climate change in autumn and early winter, the increase in streamflow is magnified. For instance, in December from the period of 2050–2100, streamflow increases by 28% in response to the climate change alone. Streamflow increases by 12% when land use/cover was converted into the future 'double rate' scenarios alone. When climate and land use/cover changes are considered simultaneously, the streamflow increases by 43% from that of the baseline period, which is greater than the effect of climate change alone. In contrast, when the direction of the effect of land use/cover change is opposite to that of climate change in spring and summer, the decrease tendency of streamflow is weakened. For instance, in March from the period of 2016–2050, the decrease rate of streamflow under the 'double rate' land use condition is reduced to –29%, which is smaller than the –39% effected from climate change alone. Moreover, with the continued and rapid expansion of developed land, the monthly streamflows during the period of 2051–2100 increase more than those during the period of 2016–2050 under the same land use condition from September to December, while the monthly streamflows during the period of 2051–2100 decrease less than those during the period of 2016–2050 under the same land use condition in other months. The same rule also applies for the streamflow between the 'current rate' and 'double rate' land use scenarios. The increase rate of monthly streamflows under the 'double rate' scenario is higher than that under 'current rate' scenario for the same period from September to December, while the decrease rate of monthly streamflows under the 'double rate' scenario is lower than that under the 'current rate' scenario from January to July.

Figures 8 and 9 show that the annual streamflows under the combined effect decrease substantially. Affected by different effect intensities, the annual streamflow values under the 'double rate' scenario decrease less than that under the 'current rate' scenario. These results show that the combined effect of climate and land use/cover changes not only influence the seasonal distribution of streamflow, but also alter the annual amount of the streamflow.

DISCUSSION

Uncertainties from the climate scenarios

On the basis of the observed data from 355 rain gauge station over China, Piao *et al.* (2010) found that southern China has undergone more and more annual-averaged precipitation because of an increase in summer and winter rainfall, while northern and northeast China have experienced less and less annual-averaged rainfall resulting from a decrease in summer and autumn precipitation since 1960. This trend may be attributed to a significant weakening of the east Asian summer monsoon, caused by a significant weakening of the component of the tropical upper-level easterly jet (TEJ) (Ding *et al.* 2008). Nevertheless, future climate scenarios from some CMIP3 or CMIP5 models predicated that the annual-averaged precipitation will increase across China for the 21st century, with a larger increase rate in northern China and a weak drying in southern China during 2011–2040 (Xu & Xu 2012; Tian *et al.* 2015). If so, this future trend suggests a slight strengthening of the Asian summer monsoon in future scenarios. However, northern China is observed to continually decrease in precipitation today (Piao *et al.* 2010). This inconsistency implies that future projections of precipitation demonstrate some uncertainties.

Moreover, uncertainties of climate scenarios are also derived from the differences in spatial scale. On a sub-regional scale (China's mainland is divided into seven sub-region), southern China will become much wetter in the 21st century based on the CMIP5 models with a resolution of $1^\circ \times 1^\circ$ grid, except in the early part of the 21st century. As for catchment-scale, it can be inferred from the $0.25^\circ \times 0.25^\circ$ CMIP5 dataset that Xinjiang Basin (belonging to southern China) will receive less and less precipitation over the whole of the 21st century under three scenarios, with decreases of -17.72% during 2016–2050 and -14.11% during 2051–2100 under scenario RCP4.5. This inference agrees with a previous study of Sun *et al.* (2013) based on CMIP3 models, which argued that Xinjiang Basin will present a decrease trend in annual-averaged precipitation in three scenarios (A1B, A2, and B1) over the 21st century.

Finally, in this paper, the climate scenarios are considered to be independent of the regional land use/cover change, and

vice versa. However, the interaction and feedback between the scenarios cannot be ignored. For example, less precipitation will contribute to a reduction in paddy land, and more water bodies will increase air moisture.

Thus, how to improve the projection of future climate scenarios still remains a major challenge. That may be dealt with by synthetically considering pollution of aerosols and dust effects and land–atmosphere interaction in regional climate simulation (Ding *et al.* 2007; Piao *et al.* 2010).

Uncertainties from hydrology model

Parameter uncertainty also causes the deviations of simulation results. During the simulation period, several model parameters (e.g., KKI, KKG) were set to be constant, ignoring their spatial-temporal variability. However, in reality, the values of these parameters may vary for different areas and seasons of Xinjiang Basin.

Owing to a lack of streamflow hydrograph separation, the three simulated streamflow components were not validated. Also, only one hydrological gauge's daily streamflow is used to calibrate and validate the Xin'anjiang model due to the scarcity of available data. Therefore, these aspects influenced the accuracy of model results in representing the hydrological characters over the entire basin.

Uncertainties from land use/cover scenarios

The land use/cover scenarios do not consider some factors that impact land use change, including economic growth and land management policy. Construction of the land use/cover scenarios were simplified based on the historical rate of developed land use change, assuming that this trend will continue. Nevertheless, the land use change trend would be non-linear. Thus, further study might use the land use dynamic model (e.g., Markov Chain model, Conversion of Land Use model, and System Dynamics model) to set up future land use/cover scenarios, which could provide more reasonable and more effective data on account of comprehensive drivers of land use/cover change (the socio-economic and natural forces).

Despite the aforementioned uncertainties and limitations, this paper can still deepen understanding of the hydrological response to future climate and land use/cover changes in Xinjiang Basin and provide some information for regional water resources planning and management in this catchment.

CONCLUSIONS

The primary objectives of this study were to analyze the effects of climate change, land use/land cover change, and their simultaneous change on future hydrologic circulation in Xinjiang Basin separately. The raster-based Xin'anjiang model was developed and utilized to simulate future streamflows under different climate scenarios and land use/cover conditions for two future periods (2016–2050 and 2051–2100), based on the CMIP5 multi-model ensemble (2016–2050 and 2051–2100). The three different climate scenarios comprised RCP4.5, RCP2.6, and RCP8.5. The three land use conditions included 'constant', 'current rate' and 'double rate' scenarios.

The effect of climate change alone induces future monthly streamflows to increase substantially in autumn and early winter, and decrease substantially in spring and summer. Although some differences in the streamflow values exist under the three climate scenarios, future streamflow changes have the same general pattern. The effect of land use/cover alone causes future streamflows to increase throughout the year. This increase mainly represents the surface runoff rather than interflow and groundwater runoff. Furthermore, the comparison of streamflow between the 'current rate' and 'double rate' conditions illustrated that rapid land development can lead to a higher increase in streamflow.

The analysis of the combined effect indicated that monthly streamflow changes are consistent with that under climate change alone, indicating that climate change plays a crucial role in future streamflows. Thus, the impact of climate change should be given more attention when predicting future streamflow. However, land use/cover change can enhance or mitigate the climate change effect. When the effects of climate and land use/cover changes are in the same (opposite) direction, the increase (decrease) trend of streamflows will be enhanced (mitigated). The combined effect of climate and land use/cover changes affects the temporal distribution of streamflow, as well as the annual amount of streamflow.

Although the uncertainties and limitations of hydroclimatic data, hydrology model, climate and land use/cover

scenarios affect the accuracy of this study to some extent, the results of this study indicate the future situation of the hydrologic cycle in Xinjiang Basin. Therefore, the results and methods have applicability for water resources management and land allocation to sustain the basin's economic growth, the natural resources, and the environment in the future. Future work will continue to optimize the uncertainty factors, including the improvement of land use/cover scenarios using the land use dynamic model, implementation of hydrograph separation to validate and model streamflow components with digital filter method, and consider the interaction between land use/cover and climate changes.

ACKNOWLEDGEMENTS

This study was financially supported by National Basic Research Program of China (No. 2012CB417006) and National Natural Science Foundation of China (No. 41371061). We acknowledge Beijing National Climate Centre for providing processed future climate datasets. The original GCMs data were provided, collected and made available by the modeling groups, the Program for Climate Model Diagnosis and Inter-comparison (PCMDI), and the World Climate Research Programme's (WCRP) Coupled Model Inter-comparison Project, respectively. We also wish to thank the anonymous reviewers and the editor for their valuable comments.

REFERENCES

Agrawal, A., Sharma, A. R. & Tayal, S. 2014 Assessment of regional climatic changes in the Eastern Himalayan region: a study using multi-satellite remote sensing data sets. *Environ. Monit. Assess.* **186** (10), 6521–6536.

Allen, R. G., Pereira, L. S., Raes, D. & Smith, M. 1998 *Crop evapotranspiration-Guidelines for Computing Crop Water Requirements*. FAO Irrigation and Drainage Paper 56. Food and Agriculture Organization of the United Nations, Rome, 300, 6541.

Arnell, N., Livermore, M. J., Kovats, S., Levy, P. E., Nicholls, R., Parry, M. L. & Gaffin, S. R. 2004 Climate and socio-economic scenarios for global-scale climate change impacts assessments: characterising the SRES storylines. *Global Environ. Change* **14** (1), 3–20.

Arora, V. K. & Boer, G. J. 2001 Effects of simulated climate change on the hydrology of major river basins. *J. Geophys. Res. Atmos.* **106** (D4), 3335–3348.

Cai, J., Liu, Y., Lei, T. & Pereira, L. S. 2007 Estimating reference evapotranspiration with the FAO Penman–Monteith equation using daily weather forecast messages. *Agric. Forest Meteorol.* **145** (1–2), 22–35.

Ding, Y., Ren, G., Zhao, Z., Xu, Y., Luo, Y., Li, Q. & Zhang, J. 2007 Detection, causes and projection of climate change over China: an overview of recent progress. *Adv. Atmos. Sci.* **24**, 954–971.

Ding, Y., Wang, Z. & Sun, Y. 2008 Inter-decadal variation of the summer precipitation in East China and its association with decreasing Asian summer monsoon. Part I: observed evidences. *Int. J. Climatol.* **28** (9), 1139–1161.

Guo, H., Hu, Q. & Jiang, T. 2008 Annual and seasonal streamflow responses to climate and land-cover changes in the Poyang Lake basin, China. *J. Hydrol.* **355** (1–4), 106–122.

Hallema, D. W., Rousseau, A. N., Gumiere, S. J., Periard, Y., Hiemstra, P. H., Bouttier, L., Fossey, M., Paquette, A., Cogliastro, A. & Olivier, A. 2014 Framework for studying the hydrological impact of climate change in an alley cropping system. *J. Hydrol.* **517**, 547–556.

Huang, J., Gao, J., Hoermann, G. & Mooij, W. M. 2012 Integrating three lake models into a phytoplankton prediction system for lake Taihu (Taihu PPS) with python. *J. Hydroinform.* **14** (2), 523–534.

Huang, J., Gao, J., Xu, Y. & Liu, J. 2015 Towards better environmental software for spatio-temporal ecological models: lessons from developing an intelligent system supporting phytoplankton prediction in lakes. *Ecol. Inform.* **25**, 49–56.

IPCC 2013 *Climate Change 2013: The Physical Science Basis. Contribution of Working Group I to the Fifth Assessment Report of the Intergovernmental Panel on Climate Change*. Cambridge University Press, Cambridge, UK & New York, NY, USA, p. 1535.

Jarsjo, J., Asokan, S. M., Prieto, C., Bring, A. & Destouni, G. 2012 Hydrological responses to climate change conditioned by historic alterations of land-use and water-use. *Hydrol. Earth Syst. Sci.* **16** (5), 1335–1347.

Kalantari, Z., Lyon, S. W., Folkeson, L., French, H. K., Stolte, J., Jansson, P. E. & Sassner, M. 2014 Quantifying the hydrological impact of simulated changes in land use on peak discharge in a small catchment. *Sci. Total. Environ.* **466**, 741–754.

Kiely, G. 1999 Climate change in Ireland from precipitation and streamflow observations. *Adv. Water Resour.* **23** (2), 141–151.

Lahmer, W., Pfützner, B. & Becker, A. 2001 Assessment of land use and climate change impacts on the mesoscale. *Phys. Chem. Earth: Part B* **26** (7), 565–575.

Legesse, D., Vallet-Coulomb, C. & Gasse, F. 2003 Hydrological response of a catchment to climate and land use changes in Tropical Africa: case study South Central Ethiopia. *J. Hydrol.* **275** (1), 67–85.

Li, Q., Bao, W., Liang, G., Qian, J. & Chen, X. 2014 Effective optimization technique for a nonlinear rainfall-runoff model. *J. Hydrol. Eng.* **19** (7), 1312–1319.

Lopez-Moreno, J. I., Zabalza, J., Vicente-Serrano, S. M., Revuelto, J., Gilaberte, M., Azorin-Molina, C., Moran-Tejeda, E., Garcia-Ruiz, J. M. & Tague, C. 2014 Impact of climate and land use change on water availability and reservoir management: scenarios in the Upper Aragon River, Spanish Pyrenees. *Sci. Total. Environ.* **493**, 1222–1231.

Lu, H. S., Hou, T., Horton, R., Zhu, Y. H., Chen, X., Jia, Y. W., Wang, W. & Fu, X. L. 2013 The streamflow estimation using the Xinanjiang rainfall runoff model and dual state-parameter estimation method. *J. Hydrol.* **480**, 102–114.

Manabe, S., Wetherald, R. T., Milly, P., Delworth, T. L. & Stouffer, R. J. 2004 Century-scale change in water availability: CO_2-quadrupling experiment. *Clim. Change* **64** (1–2), 59–76.

Moss, R. H., Edmonds, J. A., Hibbard, K. A., Manning, M. R., Rose, S. K., Van Vuuren, D. P., Carter, T. R., Emori, S., Kainuma, M. & Kram, T. 2010 The next generation of scenarios for climate change research and assessment. *Nature* **463** (7282), 747–756.

Musau, J., Sang, J., Gathenya, J., Luedeling, E. & Home, P. 2015 SWAT Model parameter calibration and uncertainty analysis using the HydroPSO R package in Nzoia Basin, Kenya. *J. Sustain. Res. Eng.* **1** (3), 17–29.

Niedda, M., Pirastru, M., Castellini, M. & Giadrossich, F. 2014 Simulating the hydrological response of a closed catchment-lake system to recent climate and land-use changes in semi-arid Mediterranean environment. *J. Hydrol.* **517**, 732–745.

Ouyang, F., Lü, H., Zhu, Y., Zhang, J., Yu, Z., Chen, X. & Li, M. 2014 Uncertainty analysis of downscaling methods in assessing the influence of climate change on hydrology. *Stoch. Environ. Res. Risk Assess.* **28** (4), 991–1010.

Piao, S., Ciais, P., Huang, Y., Shen, Z., Peng, S., Li, J., Zhou, L., Liu, H., Ma, Y. & Ding, Y. 2010 The impacts of climate change on water resources and agriculture in China. *Nature* **467** (7311), 43–51.

Rouge, C. & Cai, X. M. 2014 Crossing-scale hydrological impacts of urbanization and climate variability in the Greater Chicago Area. *J. Hydrol.* **517**, 13–27.

Sharpley, A. N. & Williams, J. R. 1990 *EPIC-erosion/productivity impact calculator: 1. Model documentation*. Technical Bulletin, United States Department of Agriculture (1768 Pt 1).

Smith, I., Syktus, J., McAlpine, C. & Wong, K. 2013 Squeezing information from regional climate change projections – results from a synthesis of CMIP5 results for south-east Queensland, Australia. *Clim. Change* **121** (4), 609–619.

Sun, S., Chen, H., Ju, W., Hua, W., Yu, M. & Yin, Y. 2013 Assessing the future hydrological cycle in the Xinjiang Basin, China, using a multi-model ensemble and SWAT model. *Int. J. Climatol.* **34**, 2972–2987.

Tian, Y., Xu, Y.-P. & Zhang, X.-J. 2013 Assessment of climate change impacts on river high flows through comparative use of GR4J, HBV and Xinanjiang models. *Water Resour. Manage.* **27** (8), 2871–2888.

Tian, D., Guo, Y. & Dong, W. 2015 Future changes and uncertainties in temperature and precipitation over China based on CMIP5 models. *Adv. Atmos. Sci.* **32**, 487–496.

Tisseuil, C., Vrac, M., Lek, S. & Wade, A. J. 2010 Statistical downscaling of river flows. *J. Hydrol.* **385** (1–4), 279–291.

Tu, J. 2009 Combined impact of climate and land use changes on streamflow and water quality in eastern Massachusetts, USA. *J. Hydrol.* **379** (3–4), 268–283.

USDA-SCS 1986 Urban hydrology for small watersheds. Technical release, Washington, DC, 55, pp. 2–6.

Van Deursen, W. 1995 *Geographical information systems and dynamic models: development and application of a prototype spatial modelling language*. Faculteit Ruimtelijke Wetenschappen, Universiteit Utrecht, The Netherlands.

Vansteenkiste, T., Tavakoli, M., Ntegeka, V., Willems, P., De Smedt, F. & Batelaan, O. 2013 Climate change impact on river flows and catchment hydrology: a comparison of two spatially distributed models. *Hydrol. Process.* **27** (25), 3649–3662.

Wisser, D., Fekete, B. M., Vorosmarty, C. J. & Schumann, A. H. 2010 Reconstructing 20th century global hydrography: a contribution to the Global Terrestrial Network-Hydrology (GTN-H). *Hydrol. Earth Syst. Sci.* **14** (1), 1–24.

Wu, C., Huang, G., Yu, H., Chen, Z. & Ma, J. 2014 Impact of climate change on reservoir flood control in the upstream area of the Beijiang River Basin, South China. *J. Hydrometeorol.* **15** (6), 2203–2218.

Xie, D., Yan, Y., Deng, H., Fang, Y. & Fan, Z. 2009 A study on the hydrological characters in the five river-catchments in JiangxiProvince. *Acta Agriculture Universitatis Jiangxiensis* **31** (2), 364–369 (in Chinese).

Xu, C. H. & Xu, Y. 2012 The projection of temperature and precipitation over China under RCP scenarios using a CMIP5 multi-model ensemble. *Atmos. Ocean Sci. Lett.* **5** (6), 527–533.

Xu, Y., Gao, X. & Giorgi, F. 2010 Upgrades to the reliability ensemble averaging method for producing probabilistic climate-change projections. *Clim. Res.* **41**, 61–81.

Yang, C., Yan, Z. & Shao, Y. 2012 Probabilistic precipitation forecasting based on ensemble output using generalized additive models and Bayesian model averaging. *Acta Meteorol. Sin.* **26** (1), 1–12.

Yao, C., Zhang, K., Yu, Z., Li, Z. & Li, Q. 2014 Improving the flood prediction capability of the Xinanjiang model in ungauged nested catchments by coupling it with the geomorphologic instantaneous unit hydrograph. *J. Hydrol.* **517**, 1035–1048.

Zhao, R. J. 1992 The Xinanjiang model applied in China. *J. Hydrol.* **135** (1), 371–381.

Zhao, G. J., Hörmann, G., Fohrer, N., Gao, J., Li, H. & Tian, P. 2010 Application of a simple raster-based hydrological model for streamflow prediction in a humid catchment with polder systems. *Water Resour. Manage.* **25** (2), 661–676.

First received 17 November 2014; accepted in revised form 15 May 2015. Available online 17 June 2015